Review



# A Review on Fusion Welding of Dissimilar Ferritic / Austenitic Steels: Processing and Weld Metallurgy

Fabio Giudice , Severino Missori , Cristina Scolaro , Andrea Sili *

Posted Date: 20 March 2024

doi: 10.20944/preprints202403.1189.v1

Keywords: dissimilar weld; arc welding; laser beam; filler metal; dilution; weld zone; solidification mode; heat affected zone.

*Review*

# A Review on Fusion Welding of Dissimilar Ferritic/Austenitic Steels: Processing and Weld Metallurgy

**Fabio Giudice [1], Severino Missori [2], Cristina Scolaro [3] and Andrea Sili [4,*]**

[1] Department of Civil Engineering and Architecture, University of Catania, 95123 Catania, Italy, fabio.giudice@unict.it
[2] Department of Industrial Engineering, University of Rome-Tor Vergata, 00133 Roma, Italy: missori@uniroma2.it
[3] Department of Engineering, University of Messina, 98166 Messina, Italy; cscolaro@unime.it
[4] Department of Engineering, University of Messina, 98166 Messina, Italy, asili@unime.it
* Correspondence: asili@unime.it

**Abstract:** Dissimilar welds between ferritic and austenitic steels represent a good solution for exploiting the best performance of stainless steels at high and low temperatures and in aggressive environments, while minimizing costs. Therefore, they are widely used in nuclear and petrochemical plants, however, due to the different properties of the steels involved, the welding process can be challenging. Fusion welding can be specifically addressed to connect low-carbon, or low-alloy steels, with high-alloy steels, which have similar melting point. Welding of thick plates can be performed with electric arc in multiple passes or in a single pass by means of a laser beam equipment. Since microstructure and consequently mechanical properties of the weld are closely related to composition, the choice of the filler metal and processing parameters, which in turn affects the dilution rate, plays a fundamental role. Numerous technical solutions were proposed for welding dissimilar steels and much research was developed on the weldment metallurgy; therefore, this article is aimed at a review of the most recent scientific literature on the issues relating to the fusion welding of ferritic / austenitic steels. Two specific sections are dedicated respectively to electric arc and laser beam welding; finally, metallurgical issues, related to dilution and thermal field are debated in the discussion section.

**Keywords:** dissimilar weld; arc welding; laser beam; filler metal; dilution; weld zone; solidification mode; heat affected zone

## 1. Introduction

Welding of dissimilar alloys allows to combine the different properties of the two parent metals with the aim of minimizing the material cost and maximizing the joint performance. The choice of the welding process and working parameters depends on physical (melting point, thermal conductivity, thermal expansion) and metallurgical properties (microstructure, thermal stability, possible formation of undesirable phases).

There are different welding procedures for dissimilar metals and, of course, fusion welding is limited only to alloys with similar melting points; for a broad classification of the processes for dissimilar materials see [1,2], in which critical factors in welding and issues regarding physical properties and metallurgical characteristics of materials were discussed. More recently, the progress and latest status on selection of welding process have been dealt in [3], collecting and hierarchically reorganizing criteria and sub-criteria of decision.

Fusion welding processes can be specifically addressed to connect low-carbon or low-alloy steels components to those made of high-alloy steels, which are better suited to low or elevated temperature service in the adverse environments typical of petrochemical and nuclear power plants (see [4] for a review on arc-welding of dissimilar steels, and [5] for a review on laser beam welding (LBW) of dissimilar metals). The usefulness of having on one side of the joint the peculiar characteristic of good

 doi:10.20944/preprints202403.1189.v1



corrosion resistance is achieved by welding at lower cost compared to the sole use of the high alloyed metal (for a summary of the common issues in fusion welding of dissimilar steels see the article of Ekeh et al. [6]).

In dissimilar steels, the final composition of the weld zone (WZ) will depend on those of the filler and the two parent (or base) metals. Usually, the filler metal has different composition than the parent metals: for welding austenitic and ferritic steels, it is generally austenitic and in several case Ni-based alloys are used, due to their high corrosion resistance. Since microstructure and consequently mechanical properties of the weld are closely related to its composition, the dilution degree plays a fundamental role in welding of dissimilar steels. Dilution is affected, in turn, by the process parameters, which therefore must be specifically determined for the welding technique adopted.

Fusion welding of dissimilar steels thick plates can be performed in multiple passes by electric arc or in a single pass using highly concentrated heat sources such as the laser beam. As is known, the heat input is decisive, not only for the weld composition and microstructure, but also for the width and metallurgical characteristics of the heat affected zone (HAZ). Numerous technical solutions and research were developed in this field, as dealt in the article by Nabavi et al. [7], in which the authors carried out an extensive review considering several pairs of dissimilar metals, such as Al / steel, Mg / steel or Cu / steel for the automotive industry, and how they can be welded optimally.

The object of the present article is to outline a review specifically addressed to the scientific literature on issues related to fusion welding of ferritic / austenitic steels. The use of the two different techniques, arc electric and laser beam, will be considered separately in two specific sections; while metallurgical topics, such as solidification mode and phase morphology, related to dilution and thermal field, will be debated in the Discussion section.

## 2. Electric Arc Welding

Arc welding processes require less plant complexity than LBW ones and result advantageous as the equipment, cheap and portable, allows in situ joints making them suitable for large structures. However, due to the high heat input transferred to the work pieces, the arc welding technique generally involves a large HAZ, excessive dilution, distortion of the welded parts, tendency to pores formation [8].

Mvola et al. [9] dealt with the general requirements for fusion welding of dissimilar ferrous metals, focusing on the gas metal arc welding (GMAW) process, in which the filler metal is fed in the form of wire and acts as an electrode. They addressed the key issues related to the weldability of dissimilar steels, which in general concern the choice of the process parameters, filler metal and dilution ratio so that both WZ and HAZ are suited for the foreseen service. Dilution is determined by the respective contributions to the WZ of the filler and the two base metals (Figure 1); therefore, in the case of carbon or low alloy steel joined with stainless steel, attention should be paid for a correct value, in order to prevent the risks of martensite formation in the weld as well as hot cracking because of an excess of P and S impurities when the carbon steel contribution prevails [10].

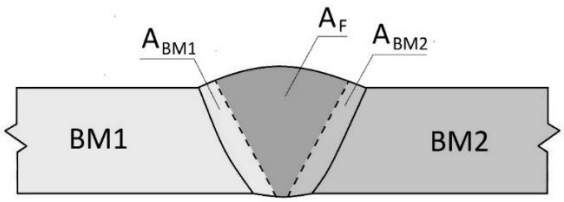


**Figure 1.** Schematic draw of a weld cross-section with indication of the weld volume per unit length $A_W = A_F + A_{BM1} + A_{BM2}$ (with $A_W$ area of the weld cross-section, $A_F$ contribution of the filler metal, $A_{BM1}$ and $A_{BM2}$ contributions of the two base metals).

In [9] the authors use the Schaeffler diagram to deduce the phases in the WZ according to its composition (expressed as weighted amounts of $\gamma$-stabilizer and $\alpha$-stabilizer elements); however, the

 doi:10.20944/preprints202403.1189.v1



update version (the WRC1992 diagram) allows a more accurate evaluation of the residual ferrite percentage in the austenitic matrix as will be covered in the Discussion section.

The effect of welding speed on dilution, microstructure and electrochemical corrosion was investigate in [11]: gas metal arc welding (GMAW) trials, under different welding speeds, between low carbon steel and AISI 304 austenitic steels were carried out. ER 309L filler metal was added in the form of consumable wire electrode, in order to compensate for Cr and Ni dilution in the molten pool. In this way the Cr and Ni compositions in the weld joints resulted higher than those in the two base metals and increased as the welding speed reduced (i.e. as the heat input increased). Corrosion performance of the weld also improved as the welding speed decreased.

An extensive review of the performance of dissimilar welds in arctic environment was carried out in [12]. This article dealt with the effects of welding processes on the weld properties, considering various aspects (such as joint preparation shape, parent metals and consumable electrode compositions), in particular with regard to the effects on low-temperature toughness.

Tungsten-inert gas (TIG) welding or gas-tungsten arc welding (GTAW) is widely used, especially in the case of thin section where the filler metal is not necessary. For a general review of the employment of this process in dissimilar steel welding, see the article of Echezona et al. [13].

Shojaati and Beidokhti [14] carried out the butt-welding of ferritic (AISI 409) / austenitic (AISI 304) plates (3 mm thick) in a single pass by GTAW. They experimented the effects of filler metals with different compositions: ER 310, ER316L, ER2209 and NiCr 80/20. The mechanical performance obtained with the ER316L austenitic filler metal represents a good compromise considering the lower cost.

Multi-pass welding is peculiar of thick components, such as boilers or furnace tubes, as it allows to deposit the filler metal, layer by layer, into the weld groove; however, it produces at each pass reheating of the previous passes [15] as well as dilution [16], which can affect the weld mechanical properties.

The multi-pass technique is widely used for dissimilar steels, as shown in the review previously cited [9]. Several articles documented the effects of multi-passes on the final microstructure: in [17] the authors studied the joint between AISI 430 ferritic steel and AISI 304 austenitic steel thin plates, performed autogenously by GTAW; in [18] the joint between low carbon steel and AISI 316 austenitic steel (using GTAW for the root pass and SMAW for the subsequent multi-passes) was investigated and compared to that produced in a single pass by SMAW.

Bahador et al. [19] experimented the effects of three different wire filler metals (ER80-Ni1, ER309L and ER NiCrMO-3 (Inconel 625)) on the final microstructure of the welds between the structural steel A516 Gr 70 and the austenitic stainless steel AISI 316 L, produced by GTAW with pure Ar as shielding gas. Since the plates were 12 mm thick, their edges were beveled with an angle of 45° and the multi-pass technique was adopted. Among the three different filler metal experimented, the third (Inconel 625) was found to be the most suitable because it showed the highest tensile strength and best hardness distribution in the weld cross section.

The effects of GTAW multi-passes and different bevel angles of the V-grove on dissimilar butt-positioned plates, made of pipeline steel (API X52) and super duplex stainless steels (SDSS 25Cr7Ni) were analyzed in [20]. Based on previous articles [21,22], the choice of welding parameters and filler metal (ER2594) raised from a compromise, taking into a account how microstructure is crucial for corrosion resistant. The results given in [20] was focused on the effects on corrosion behavior of the welds, showing that with a bevel angle of 75° slower cooling rates give rise to the microstructure best suited to reducing corrosion rate.

In a recent article [6], the authors investigated the dissimilar joints between DSS 32205 duplex stainless steel and API 5LX60 steel, obtained with GTAW and ERNiCrMo-3 filler metal, in order to achieve good performance for offshore applications.

The TIG process activated by a fusible flux (A-TIG) was successfully experimented by Zhang et al. [23] for welding Q245R mild steel to AISI 321 austenitic stainless steel. The surface of the metals to be welded was coated by a thin layer of flux, consisting of a mixture of oxides, which, by capturing electrons, improves the arc performance. It resulted in an increased weld penetration and no defects,

 doi:10.20944/preprints202403.1189.v1



such as gas holes, inclusions and cracks. Consequently, the welds showed better strength and toughness than those obtained with conventional TIG welding.

Yilmaz and Tumer [24] considered the joining between the low alloy steel AH36 and the austenitic stainless steel AISI 304 L with flux-cored arc welding (FCAW). This process uses a consumable tubular electrode which continuously fed the weld, whose core produces a flux of liquid slag protecting the melting pool. The authors investigated the effects of the shielding gas composition, observing that the impact performance of the weldment decreases if the $CO_2$ content increases; furthermore, it also involves an increase in the austenitic volume and thus a reduction of the δ-ferrite percentage in the WZ.

In shielded metal arc welding (SMAW) the electrode plays a significant role in weld quality. In fact, in addition to providing the filler metals, the decomposition of the coating produces the slag, which acts at the interface with the molten pool, and the gaseous protection from oxidation [25]. The article of Bhandari et al. [26] was aimed at developing a SMAW process for joining dissimilar plates (SA516 and AISI304L), using coated electrodes. Pratiwi et al. recently published [27] an experimental study with the aim of optimizing the SMAW process parameters for welding ASTM A36 mild steel to AISI 316 austenitic steel.

The submerged arc welding process (SAW) was also experimented to deposit, on a plate of 18MND5 low-alloy steel (similar to ASTM A533 grade B or DIN 1.6308), a layer of 309L stainless steel [28]. A granular fusible flux of silica, fluorides and other oxides protects the molten pool and the arc zone from atmospheric contamination. In this process, only one layer was deposited so that its microstructure, which is not modified by any thermal effects due to subsequent passes, allows to document the solidification mode of the austenitic weld bead.

Any misalignments of the electric arc with respect to the axis of the joint can lead to an asymmetric contribution by the two base metals giving rise to an incorrect dilution. In some case, the buttering technique at the carbon steel side (Figure 2), with the use of a proper composition of the filler metal, is recommended to compensate for the differences in composition between the two metals to be welded. However, it is always necessary to consider the effects of all the parameters that characterize the welding process on which dilution depends.

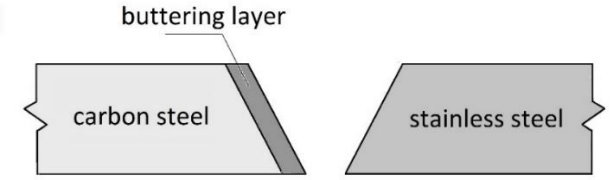


**Figure 2.** Schematic draw of two butt-positioned plates with the buttering layer at the carbon steel side.

In [26], to compensate dilution with a layer rich of Ni and Cr, SS309L electrodes were used for buttering the carbon steel edge; subsequently, SS308L electrodes were used in SMAW of two dissimilar plates (SA 516 and AISI 304L). Mechanical test showed that the ultimate tensile strength of the welds increased with the amount of $TiO_2$, $SiO_2$ and $CaF_2$ in the electrodes coating, while the presence of CaO, $SiO_2$ and $CaF_2$ caused a significant decrease.

In [29] the buttering technique was used in GTAW of two dissimilar plates (A508 Grade 3 and AISI 304 L), which were butt-positioned and prepared with a conventional V groove. The low alloy steel side was buttered by ERNiCr-3 filler wire; anyway, islands of martensite and complex alloy carbides were observed near the fusion line boundary at the low alloy steel side. The authors also experimented GTAW between the same plates, butt-prepared with a narrow gap and without buttering. This preparation required less heat input during welding; regarding metallurgical and mechanical characteristics, the weldment showed better performance than that obtained with the buttering preparation.

More recently, Asadollahi et al. [30] have investigated the effects of three different filler metals (ER308L, ER309L and ERNiCr3) in GTAW of the dissimilar plates API 5L X65 and AISI 304 L (10 mm

 doi:10.20944/preprints202403.1189.v1



thick). Before welding, the ferritic steel edge was prepared with a buttering layer (6 mm thick), through GTAW passes with ERNiCr3 filler wire. First, if compared to non-buttered welds, the results of metallographic investigations demonstrated that buttering hinders the formation of a brittle martensitic/bainitic layer at the fusion line. The results of mechanical tests showed that the best properties were achieved in the sample welded with ERNiCr3 filler metal.

**3. Laser Beam Welding**

Nowadays, LBW has also become widespread for dissimilar metals due to the high degree of automation and accurate energy control, mainly by means of $CO_2$ or Nd:YAG laser apparatus; while fiber laser technology have only recently caught on [31]. The high level of energy concentrated in a small volume allows to work at higher welding speed than arc welding, obtaining with a single pass narrow and deep joints in thick steel plates. Another advantage over conventional arc welding is the small size and accuracy of the beam spot that gives rise to reduced sizes of both WZ and HAZ. In this regard, the beneficial effects on mechanical properties of both rapid solidification in the WZ and small width of the HAZ were experimented in mild steel / austenitic steel joints produced by LBW [32].

Even if the formation of embrittling intermetallic compounds can occur, this problem is smaller in LBW than in conventional arc welding [2]. However, due to the rapid solidification of the molten pool, LBW generally shows a high tendency to solidification cracking, which can be controlled by a careful selection of the filler metal and the welding parameters, as will be debated in the Discussion.

The high production rate makes LBW suitable for high productivity in series; furthermore, the investment resources in laser equipment are well compensated, due to the good performances and cost savings achieved for different pairs of dissimilar metals [5].

Regarding the applications in the field of dissimilar materials, LBW has been considered in power generation system as well as in the automotive industry which requires appropriate methods for joining steels and light alloys. In fact, the small size of the weld pool reduces diffusion and lowers the mixing between the two materials compared to traditional electric arc techniques, as amply demonstrated by the scientific literature on this subject [33,34].

With a suitable choice of the welding parameters, the laser beam produces a narrow and deep plasma zone, the so called “keyhole”, which in turn solidifies as a narrow weld bead with a reduced width of the HAZ. Furthermore, the keyhole mode produces rapid cooling and consequently reduces the exchanges of alloying elements by diffusion between WZ and parent metals. In these conditions, AISI 304 stainless steel thick plates, 12 mm thick, can be welded in a single pass without any filler metal [35].

In recent years LBW has been utilized for joining ferritic / austenitic dissimilar steels and some researchers addressed their efforts in butt-joining thin sheets without filler metals: AISI 1010 to AISI 321 in [36], AISI 1010 to AISI 304L in [37] and 9Cr-1Mo-V-Nb to 316 L(N) in [38], S235JR to AISI 316L in [39]. However, in absence of a filler metal with composition such as to compensate for the absence of alloying elements in carbon steel, dangerous martensitic microstructures were observed in the welds.

In [40] Hamada et al. performed an autogenous LBW of Docol S355 to AISI 201 medium-Mn stainless steel. The presence of martensitic structures was highlighted in the welds and therefore post welding heat treatment resulted necessary to homogenize microstructure, relieve residual stress and therefore improve mechanical performances.

Recently, in [41] the authors have investigated the effects of two different heat inputs in LBW between S355 low alloy steel and AISI 316 austenitic stainless steel. Two dissimilar plates (5 mm thick) were butt-positioned and autogenously welded with laser beam power constant at two different welding speeds. Metallographic investigation showed in the WZ a martensitic microstructure with 5% of austenite that become fully martensitic when the heat input increase (i.e. the welding speed decreases). Higher values of micro-indentation hardness were measured in the case of fully martensitic microstructure.

The opportunity of post-welding heat treatments was also considered in literature: Prabakaran and Kannan, using process parameters optimized in a previous work [42], performed LBW between

 doi:10.20944/preprints202403.1189.v1



AISI 1018 and AISI 316 thin sheets, in a single pass and without filler metal, and then carried out post-welding heat treatment at 960°C [43]. In this way a microstructure of pure martensite with no carbide precipitates was obtained in the WZ, resulting in an improved mechanical strength.

Liu et al. [44] considered the autogenous LBW between AH36 and AISI 304 thin sheets (3 mm thick) and showed, trough metallographic investigation and numerical simulation, that changes of the laser beam offset (Figure 3) affect the melt flowing, the shapes of fusion boundaries and consequently the final chemical composition of the weld and its microstructure.

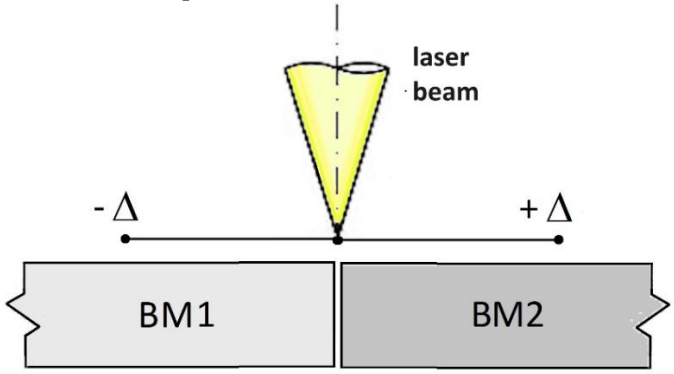


**Figure 3.** Sketch of the laser beam offset considered for research purpose (Δ=0.5 mm [44]).

The issues related to the thinness of the laser beam, which implies very strict requirements on machining and assembling of workpiece, can be overcome with hybrid laser-arc welding (Figure 4). Some authors explored the synergic effects of a welding torch and a laser beam which travel at few millimeters of distance along the same axis. The results given in literature (see for example Li et al. [45] for welding thick plates of mild steel, or Spena et al. [46] for welding Mn steel to dual phase steel) can be considered preparatory for applications in welding ferritic / austenitic dissimilar steels. In this regard the work of Zhang et al. [47] is exemplifying, as it demonstrates how an acceptable 20 mm thick weld between dissimilar EH36 mild steel and 316L austenitic steel can be obtained by optimizing the welding parameters of a narrow-gap hybrid laser-arc welding process.

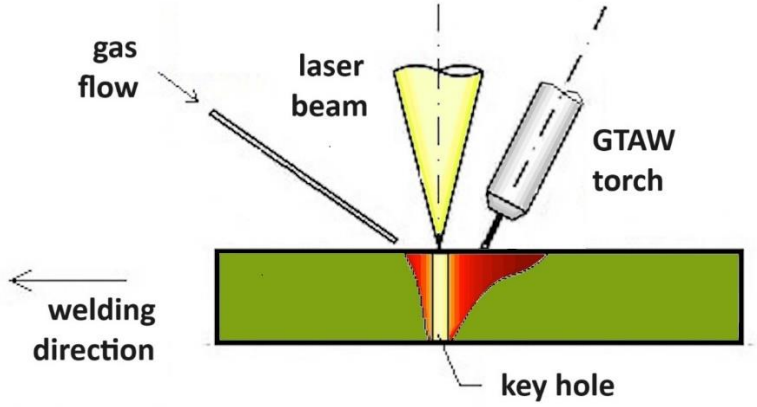


**Figure 4.** Sketch of hybrid laser-arc welding setup [48].

It is known that in LBW processes the use of filler wire implies stringent requirements for positioning [49]. On the other hand, laser beam allows for deep autogenous welding of thick plates; however, in the case of dissimilar metals, the use of an appropriate filler metal is crucial to compensate for dilution and achieve good weld performance.

An alternative way could be the addition of filler metal in form of consumable inserts, placed between the edges of two butt-positioned plates. This solution was adopted in [48] for LBW two plates of carbon steel clad with austenitic steel, achieving good results with a suitable choice of the welding parameters (Figure 5).

 doi:10.20944/preprints202403.1189.v1



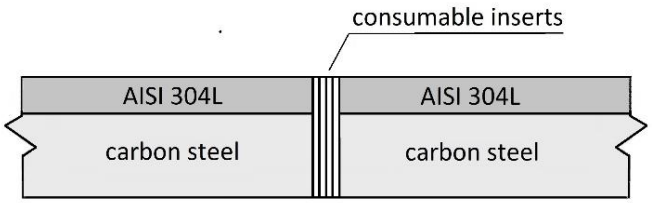


**Figure 5.** Preparation of clad steels for LBW [48].

Fiber laser technology have only recently caught on for a beam of outstanding optical quality and a precise welding action [31]. High-power fiber laser allows the beam to be split in multiple beams (each one with intensity sufficient to work in the keyhole mode), which can be shaped in a pre-defined pattern of multiple spots to reproduce the actual joint configuration.

Although there are references in the literature to the multi-beam welding between stainless steel or between carbon steel and aluminum sheets, it is worth thinking that this technique could be useful also for joining dissimilar steels. In [50], the authors demonstrated that it is possible to produce a bead with rectangular cross-section by correctly choosing the spot configuration and the working parameters. For a row of multiple spots, they obtained equal penetration depth if the edge spots have 5%–10% more power than the center spots. Beam splitting, produced by a high-power fiber laser apparatus, was used to butt-weld four stainless sheets placed in a complex geometry [51]. The pattern utilized for the multiple beams was side-by-side, characterized by three spots for each of the three joints to be welded. Furthermore, Cui et al. successfully performed LBW of steel/Al lapped joints by means of a dual-beam with a side-by-side configuration (Figure 6) [52]. These results seem encouraging for the use of the multiple spot technique in welding dissimilar steels.

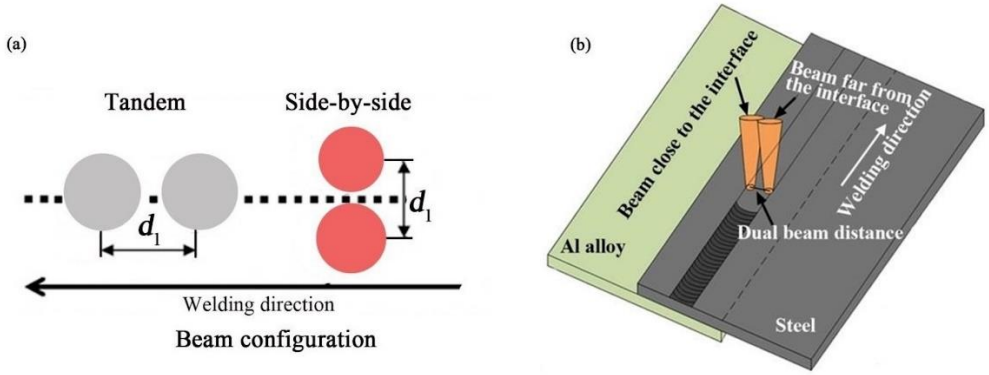


**Figure 6.** a) Tandem and side-by-side configurations; b) Setup of the side-by-side configuration (reproduced from [52]).

## 4. Discussion

Physical and mechanical properties are not the same in the weld and parent metals. For example, the linear thermal expansion coefficient $\lambda$ (°C$^{-1}$) varies from about 13·10$^{-6}$ for carbon steel to 17·10$^{-6}$ for AISI 304 austenitic steel and 10·10$^{-6}$ for AISI 430 ferritic steel; heat conductivity k (W/(°C·m)) from 45 for carbon steel to 16 for AISI 304 and 25 for AISI 430. The difference in coefficients of thermal expansion between ferritic and austenitic steels gives rise to distortions or, when prevented, to thermal stresses, as shown by the numerical simulation carried out in [53,54]; moreover, recent experimental measurements and numerical simulations were performed investigating the effects of cooling and heating cycles during service [55].

Anyhow, in dissimilar welding it is more difficult to control the composition of the molten zone, which plays a fundamental role in determining microstructure and mechanical properties and therefore in the weldability of the parent metals involved. Attention must be paid to the presence of elements forming carbides or intermetallic compounds, detrimental to mechanical performance [56]

 doi:10.20944/preprints202403.1189.v1



and to corrosion resistance [57]. In particular, when welding dissimilar ferritic / austenitic steels, carbon steel of low quality could provide elements, such as sulfur and phosphorus, which segregates at the boundaries of the austenitic dendrites in the WZ, generating low-melting eutectic phases and giving rise to solidification cracks [58,59].

To avoid these risks, the WZ composition must be balanced by the addition of an adequate filler metal, whose effects depends on the dilution ratio. The following relationships give the dilution ratios respect to the filler metal ($d_F$) and to the two base metals ($d_{BM1}$ and $d_{BM2}$):

$$d_F = A_F / (A_F + A_{BM1} + A_{BM2}), \quad (1)$$

$$d_{BM1} = (A_{BM1}) / (A_F + A_{BM1} + A_{BM2}), \quad (2)$$

$$d_{BM2} = (A_{BM2}) / (A_F + A_{BM2} + A_{BM2}), \quad (3)$$

Where $A_F$, $A_{BM1}$ and $A_{BM2}$ represent the volumetric quantities of the filler metal and the two base metals respectively, which are reduced by one dimension into area terms under the assumption that the cross-sectional areas do not vary along the weld bead length [10].

Once the dilution values are known, the WZ composition results from a weighted mass balance. Then its microstructure can be estimated, based on $Cr_{eq}$ and $Ni_{eq}$ compositions, through the Schaffler diagram (based on the equivalent compositions expressed as percentages by weight: $Cr_{eq} = Cr + 1.5 \cdot Si + Mo + 0.5 \cdot Nb$ and $Ni_{eq} = Ni + 30 \cdot C + 0.5 \cdot Mn$), or by means of the more recent evolution WRC 1992 diagram ($Cr_{eq} = Cr + Mo + 0.7 \cdot Nb$ and $Ni_{eq} = Ni + 35 \cdot C + 20 \cdot N + 0.25 \cdot Cu$). They are currently used by many researchers (see [9,60,61] for the Schaffler diagram and [62–64]) for the WRC 1992 diagram).

When ferritic / austenitic dissimilar steels are welded without filler metals, dilution in the WZ gives rise to compositions within the martensitic range (Figure 7).

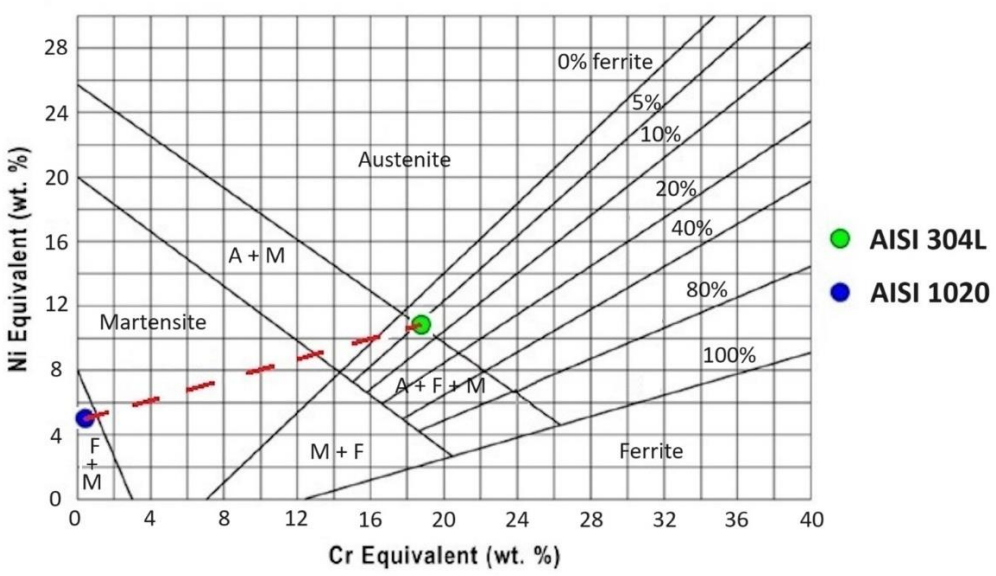


**Figure 7.** Schaeffler diagram (adapted from [61]): the red dashed line represents the composition range of the WZ in relation to the dilution ratio.

In the case of dissimilar welding between AISI 1020 and AISI 304L thin sheets without filler metal (Figure 8), Scutelnico et al. [37] documented the formation of a hard martensitic microstructure in the WZ, as shown in Figure 8 by the results of Vickers hardness measurements, performed along a traverse on the joint cross-section from the CS-side (AISI 1020 mild steel) to the SS-side (AISI 304L austenitic steel).

 doi:10.20944/preprints202403.1189.v1



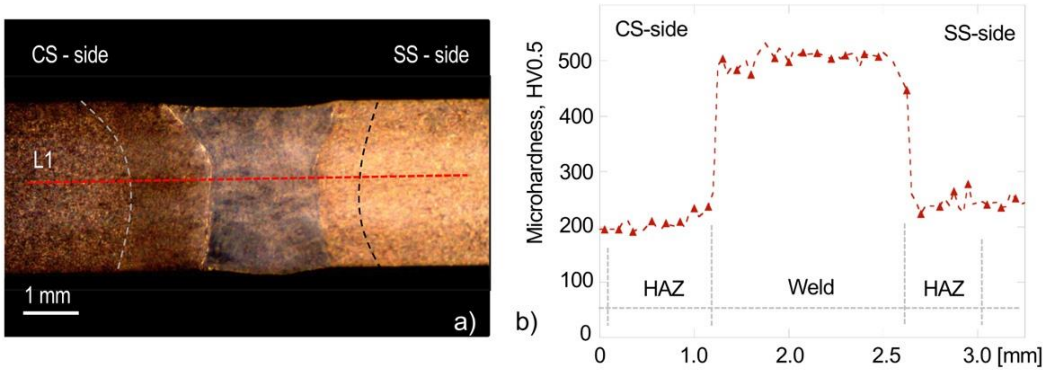


**Figure 8.** Hardness analysis. (a) Location of the microhardness imprint line L1 on the joint section; (b) microhardness profile along the analyzed line (reproduced from [37].

For compositions in the ferritic austenitic field, solidification takes place following the modes listed in Table 1, according to [65–67], even if some authors report slightly different limit values [7] Nabavi.

**Table 1.** Solidification modes of stainless steels.

| Composition ranges[1, 2] | Solidification modes | Sequence of transformations |
|---|---|---|
| $Cr_{eq}/Ni_{eq} > 2.0$ | F (ferritic) | $L \rightarrow L + \delta \rightarrow \delta$ |
| $1.5 < Cr_{eq}/Ni_{eq} < 2.0$ | FA (ferritic-austenitic) | $L \rightarrow L + \delta \rightarrow L + \delta + \gamma \rightarrow \delta + \gamma$ |
| $1.37 < Cr_{eq}/Ni_{eq} < 1.5$ | AF (austenitic-ferritic) | $L \rightarrow L + \gamma \rightarrow L + \delta + \gamma \rightarrow \gamma + \delta$ |
| $Cr_{eq}/Ni_{eq} < 1.37$ | A (austenitic) | $L \rightarrow L + \gamma \rightarrow \gamma$ |

In general, the austenitic microstructure tends to be less susceptible to solidification cracking when the solidification mode is FA, characterized by primary δ-ferrite, while the other solidification modes show a worse behavior. The main reason is the presence of ferritic–austenitic boundaries at the solidification end, which resist wetting by liquid films containing low-melting phases responsible for hot cracking [68]. In this case, about 5% of retained primary ferrite is usually considered as a requirement for an austenitic weld to avoid solidification cracking [69].

Zhou et al. [70] demonstrated that, in an austenitic WZ, the presence of residual δ-ferrite with skeletal morphology prevents also hydrogen embrittlement. However, concentrations of ferrite of about 10 % and above favor selective attack by some corrosive media; moreover, when working temperatures are in the 550-900°C range, primary ferrite could decompose into carbides and phases detrimental for mechanical properties, such as ductility, impact toughness, creep strength as well as corrosion resistance [71]. For these reasons, its content in the weld metal should be limited [72].

The content of primary ferrite is affected by the welding heat input [70]. For high heat input, and consequently slow cooling rate, the solidification time is getting longer and thus the initial content of ferrite is high, however the duration of the transformation $\delta \rightarrow \gamma$ is prolonged leading to a reduction of the primary ferrite content, caused by increased formation of austenite [24]. The opposite occurs when the heat input is lower and cooling rate higher, as clearly shown in [73] where it was observed that the primary ferrite content in the FZ increased with decreasing heat input.

However, if cooling rate exceeds a limit value, the FA mode could be completely cancelled out and the austenitic molten pool could solidify as primary austenite, instead of as primary ferrite [74].

Regarding the morphological aspects, the ratio between the temperature gradient (G) and solidification rate (R) represents a useful parameter. The G/R value is high close to the fusion line, where the solidification is planar / cellular, while decreases approaching the weld centerline where an equiaxed microstructure occurs under a sufficient undercooling [75]. The presence of alloying elements favors the formation of the dendritic morphology, as shown for three representative metals in Figure 9, taken from [67]. Note that X65C carbon steel, being low in alloying elements, undergoes planar solidification over a wide range of G/R values.

 doi:10.20944/preprints202403.1189.v1



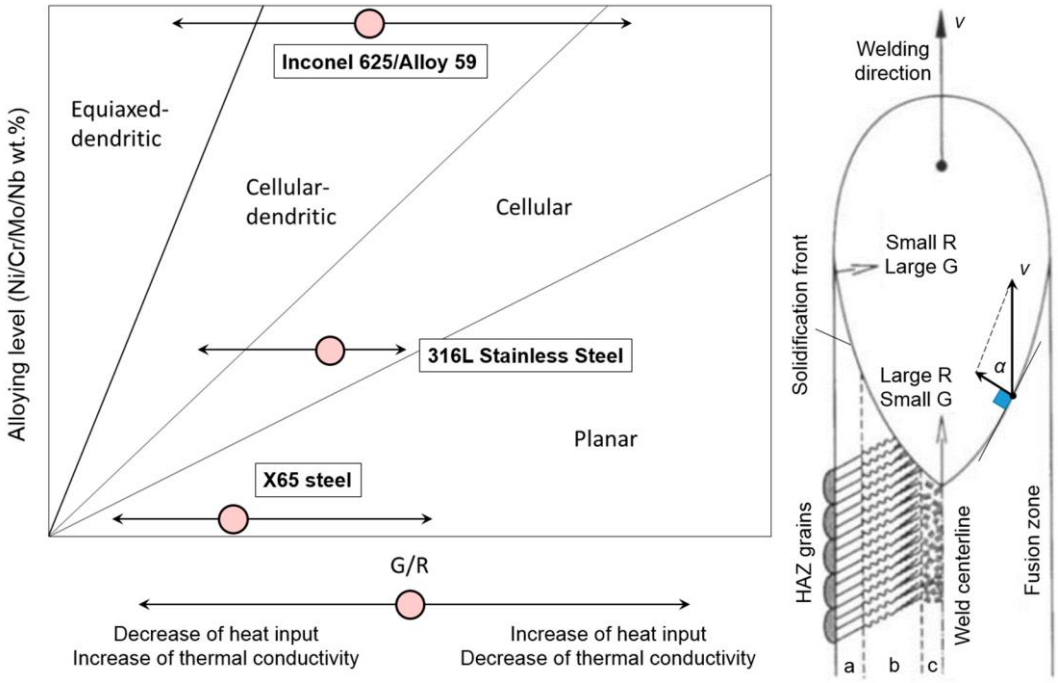


**Figure 9.** On the left, solidification modes for three representative metals, according to the ratio G/R and alloying elements content; on the right, sketch of the solidification morphology around the molten pool: a) cellular, b) cellular-dendritic and c) equiaxed-dendritic solidification mode). Reproduced from [67].

For an in-depth microstructural study of a carbon steel / austenitic steel weld, see the reference [28] already cited in the arc welding section. In this article, the authors published an optical micrography of the weld cross section, which shows that on the carbon steel side the original bainitic microstructure becomes martensitic in the HAZ, followed on the weld side by a narrow layer of martensite, then by a fully austenitic zone and finally by the typical microstructure of the austenitic stainless steel with 18% of Cr and 9% of Ni, characterized by a γ matrix with residual ferrite (Figure 10a). These observations are confirmed by the composition profiles of Fe, Ni and Cr, obtained with EDS measurements and showed in Figure 10b: starting from the HAZ, first the profiles are flat, then sharp gradients of the alloying elements characterize the transition towards the homogeneous mixing in the molten pool, which the author determined in proportion of 20% base metal and 80% filler metal.

 doi:10.20944/preprints202403.1189.v1



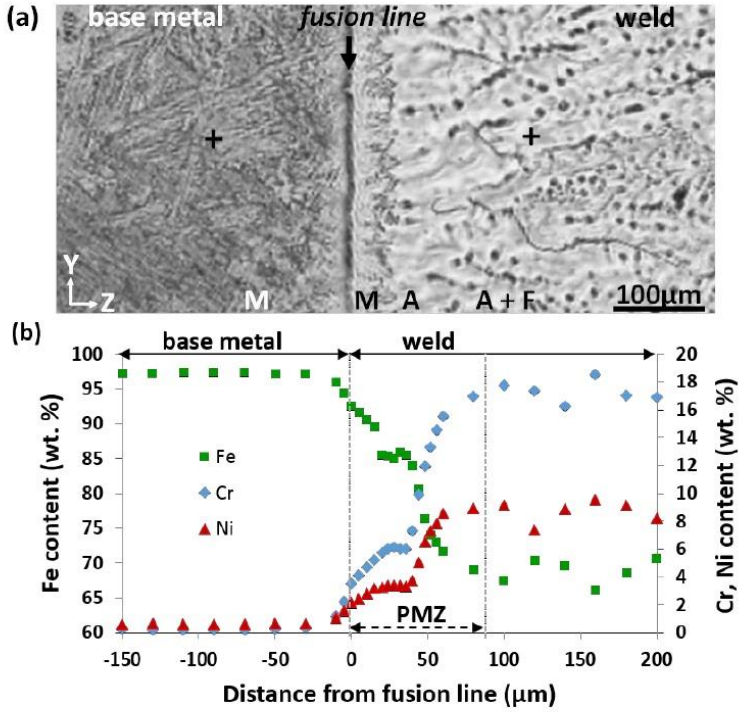


**Figure 10.** Weld cross section: carbon steel (base metal) austenitic steel (weld): a) optical micrograph with indication of microstructure (M martensite, A austenite, A + F austenite and ferrite); b) composition profiles of Fe, Ni and Cr vs. the distance from the fusion line. Reproduced from [28].

In this regard, starting from the fusion line, Mas et al. [28] documented the following sequence of solidification: cellular A mode ($\gamma_1$), cellular AF mode ($\gamma_1$, $\delta$), dendritic FA mode ($\delta_1$, $\gamma_2$, $\gamma_2$) with evidence of skeletal primary ferrite (Figure 11).

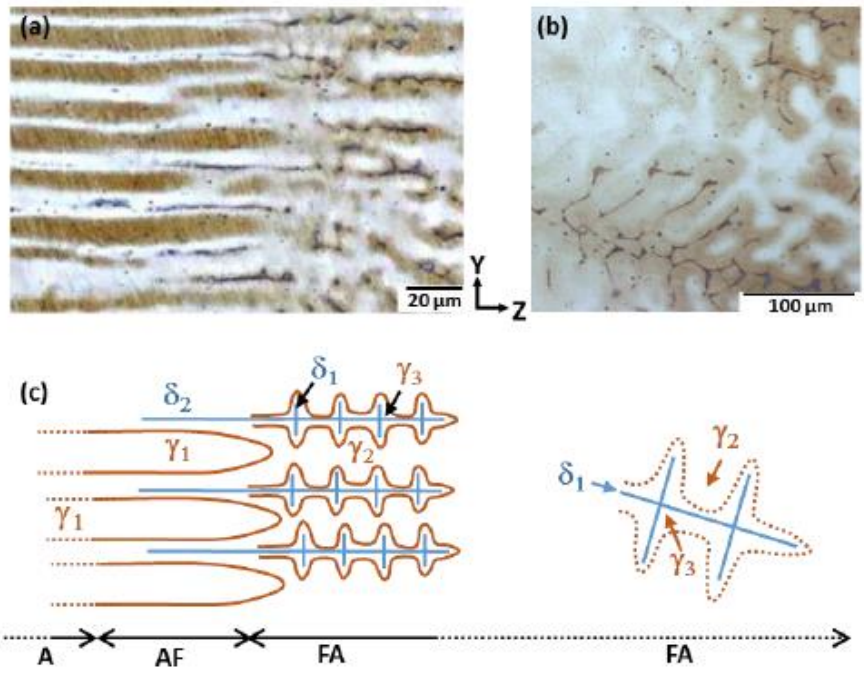


**Figure 11.** Evolution of the solidification mode of the weld (austenite in dark/light brown and ferrite in black): a) microstructure close to the fusion line; b) microstructure far from the fusion line; c) evolution of the solidification mode. Reproduced from [28].

 doi:10.20944/preprints202403.1189.v1



In general, welding speed has important effects on cooling rates as investigated in literature by finite elements methods [76], using a commercial software [77], or by a new analytical model experimentally fitted on the weld cross-section contour, which was presented in [78] and validated in [79]. It would be appropriate to find articles that specifically deal with the effects of welding speed on cooling rates in welds between dissimilar steels. Anyway, the simulations of thermal fields produced during LBW of two thick AISI 304L plates, with AWS 309L inserts as filler material, carried out in [63], can also provide useful indications for welding dissimilar ferritic / austenitic steels; in fact, although the cooling rates could influence the ferrite - austenite transformations, for the welding conditions considered, they do not reach values that affect the expected percentage of primary ferrite in the weld, according to the WRC 1992 diagram.

The effects of re-heating due to multi-pass on the WZ and HAZ of the joint between low carbon steel and AISI 316 steel was studied in [18]. The authors documented some differences in the microstructure between single-pass and multi-pass welding. In the first case, the WZ microstructure is characterized by the transformation from cellular to columnar and equiaxed dendrites; while, in the second case, the columnar dendrites are extended from the fusion line of a weld pass towards the subsequent one. Because of the recrystallization processes generated by the heat input of the various passes, the multi-pass welding showed grain refinement and higher hardness on carbon steel side than single pass welding.

Regarding the HAZ, on the austenitic side the occurrence of conditions that favor sensitization to intergranular corrosion must be considered. This phenomenon is due to Cr atoms depletion near the austenitic grain boundaries, caused by Cr-carbide precipitation during welding within the range 400-800°C (for a review on this topic see [80]). At a given temperature, the higher the carbon content the shorter the precipitation time: for example, in an austenitic steel containing 0.056% of Carbon, at 700°C, 7 minutes are needed for sensitization ([72] Weman 2003). Carbide precipitation is easily detectable, as it produces increases in hardness, and can be recovered through heat treatment at the homogenizing temperature in the range 1000-1100°C, followed by a reduction in hardness [81].

During LBW of AISI 304 thick plates performed in [63], the conditions favorable for sensitizing were not reached, because the exposure time within the critical temperature interval resulted to be only few seconds, as shown by the simulation of the thermal fields.

Conversely, Dae et al. [82] carried out multi-pass of GTAW on butt-positioned thick plates of dissimilar ASTM 335 P92 martensitic steel / AISI 304 austenitic steel, using Alloy 82 as filer metal. Their work was aimed at developing a model that can accurately predict the zone with the most serious degree of sensitizing: the results indicated that sensitization mainly occurred on the austenitic side, in the lower half of the joint at a distance of approximately 7.5 mm from the WZ boundary.

On the ferritic side of dissimilar steels, it is likely to encounter a microstructure with high hardness, such as martensite and bainite, depending on the process setup and the adopted welding parameters, which determine the heating in the austenitic field and the subsequent rapid cooling [83]. However, it should be considered that ferritic steels have a higher carbon content than austenitic steels, in which carbon concentration is usually limited to avoid sensitizing phenomena. Therefore, the carbon gradient favors the diffusion of this element towards the austenitic side; furthermore, the solubility of this element is higher in austenite than in ferrite, while the diffusion coefficient is much higher in ferrite. These factors together generate a strong carbon diffusion from the ferritic base steel to the austenitic WZ, resulting in a carbon depletion on the ferritic side near the fusion line and a consequent local reduction in hardness, which can affect a zone wide about 50-100 μm [84].

A difference in chemical composition between base and weld metals can be created intentionally, as done in [85] by choosing a CN 23/12 Mo-A austenitic filler metal for GTAW two ASTM A335 P91 martensitic steel plates. The welding trial was performed in a single pass to eliminate the consequence of re-heating. In this way the authors investigated the effects of the heat input and pre-welding thermal treatments on the width of the decarburized layer. In [86], the same ASTM A335 P91 martensitic steel was joined to AISI 304L austenitic steel by multi-passes of GTAW using two different filler metals (309L-16L or ERNiCr-3). The weldability of this pair of dissimilar steels was studied by microstructural investigations of the weld metal and HAZ, as well as mechanical tests, determining

 doi:10.20944/preprints202403.1189.v1



that ERNiCr-3 is the preferred filler. Moreover, the authors ascertained that the weld microstructure consists of austenitic dendrites with a minor fraction of ferrite in the interdendritic spaces.

## 5. Conclusions and Future Directions

Arc welding and LBW processes are currently used for joining dissimilar steels. Progress in this field has developed over the last 20 years, as highlighted by the vast scientific production in literature.

Many researchers have directed their efforts to setup the fusion welding process and optimize the working parameters. In fact, when welding dissimilar steels, the choice of the process is crucial, since dilution, on which depend the weld composition, is affected by the heat input.

Different arc welding techniques, such as GTAW, GMAW, FCAW, SMAW or SAW, have been object of research. Each of them was finalized by the authors for specific purposes and led to different evaluations, regarding both the process setup and the mechanical and metallurgical characterization of the welds.

Even if LBW requires greater equipment complexity than arc welding, it has proven to be largely advantageous for the high-quality of welds, due to the high concentration of energy and the automatism of the welding system which allows better control of the working parameters. In this way, it is easier to limit any misalignments that can alter the degree of dilution in the weld, although the thinness of the laser beam implies very strict requirements in machining and assembling of the workpiece, which can be overcome by hybrid laser-arc welding.

With regard to dilution and metallurgical issues, differences in composition between two different base metals need to be balanced by a proper composition of the filler metal, with the purpose of obtaining in the weld an austenitic microstructure with a little amount of residual δ-ferrite, which is the best condition to prevent hot cracking.

Although many articles have been produced, several topics, such as solidification modes, diffusion and solid phase transformations are still worthy of further investigations.

Another important aspect to investigate is the simulation of the thermal fields as a function of the process parameters. This would allow researchers to make metallurgical and mechanical predictions about the generation of residual stresses as well.

Not to mention the improvement of laser welding processes, for example with the use of consumable inserts as filler material or with the refinement of spot welding by fiber laser. Considering the advantages of the multi spot technique, the development of double laser systems, with an up and down setup, could be also desirable for welding very thick plates in a single pass.

**Author Contributions:** Conceptualization, F.G., S.M., C.S. and A.S.; methodology, F.G., S.M., C.S. and A.S; investigation, F.G., S.M., C.S. and A.S.; data curation, F.G., S.M., C.S. and A.S.; writing—original draft preparation F.G., S.M., C.S. and A.S.; writing—review and editing, F.G., S.M., C.S. and A.S.; visualization, F.G., S.M., C.S. and A.S.; supervision, F.G., S.M. and A.S. All authors have read and agreed to the published version of the manuscript.

**Funding:** This research received no external funding.

**Data Availability Statement:** No new data were created; therefore, data sharing is not applicable to this article.

**Conflicts of Interest:** The authors declare no conflicts of interest.

## References

1. Kah, P.; Shrestha, M.; Martikainen, J. Trends in joining dissimilar metals by welding. Applied Mechanics and Materials **2014**, 440, 269-276
2. Martinsen, K.; Hu, S.J. Hu, Carlson, B.E. Joining of dissimilar materials CIRP Annals – Manufacturing. Technology **2015**, 64, 679–699 http://dx.doi.org/10.1016/j.cirp.2015.05.006
3. Soltan, H.; Omar, M. A roadmap for selection of metal welding process: a review and proposals. **2022**, Welding in the World, 66, 2639–2675 https://doi.org/10.1007/s40194-022-01379-1
4. Maruyama, T. Arc welding technology for dissimilar joints. Welding International **2003**, 17, 276–281 https://doi.org/10.1533/wint.2003.3113

5. Boumerzoug, Z. A review: welding by laser beam of dissimilar metals, Aspects Min Miner Sci **2021**, 8, 916-920 https://doi.org/10.31031/AMMS.2021.08.000683
6. Ekeh, T.D.; Lawal, F.T.; Osoba, L.O.; Amuda, M.O.H. Microstructure and mechanical properties of dissimilar welds of duplex and API steel for offshore applications. International Journal of Materials Technology and Innovation **2023**, 3, 2, 80-91 https://doi.org/10.21608/ijmti.2023.207906.1084
7. Nabavi, S F.; Farshidianfar, A.; Dalir, H. A comprehensive review on recent laser beam welding process: geometrical, metallurgical, and mechanical characteristic modeling, Int J Adv Manuf Technol **2023**, 129, 4781–4828 https://doi.org/10.1007/s00170-023-12536-1
8. Abioye, T.E.; Olugbade, T.O.; Ogedengbe, T.I. Welding of dissimilar metals using gas metal arc and laser welding techniques: a review. Journal of Emerging Trends in Engineering and Applied Sciences 2**017**, 8, 6, 225-228
9. Mvola, B.; Kah, P.; Martikainen, J. Dissimilar ferrous metal welding using advanced gas metal arc welding processes. Rev. Adv. Mater. Sci. **2014**, 38, 125-137
10. DuPont, J. N. Dilution in fusion welding, in *Metals Handbook*,1st ed. Lienert, T. J.; Babu, S. S.; Siewert, T. A.; Acoff, V. L. Eds. ASM, Materials Park, Ohio US, 2011, Volume 06A, pp. 115-121
11. Abioye, T. E.; Ariwoola, O.E.; Ogedengbe, T.I.; Farayibi, P.K.; Gbadeyan, O.O. Effects of welding speed on the microstructure and corrosion behavior of dissimilar gas metal arc weld joints of AISI 304 stainless steel and low carbon steel. Materials Today: Proceedings **2019**, 17, 871-877
12. Mvola, B.; Kah, P.; Martikainen, J.; Suoranta, R. Dissimilar welded joints operating in sub-zero temperature environment. Int J Adv Manuf Technol **2016**, 87, 3619–3635 https://doi.org/10.1007/s00170-016-8711-4
13. Echezona, N.; Akinlabi, S. A.; Jen, T. C.; Fatoba, O. S.; Hassan, S.; Akinlabi, E. T. Tig welding of dissimilar steel: a review. In Advances in Manufacturing Engineering, Lecture Notes in Mechanical Engineering, M. Awang and S. S. Emamian (Eds.), publisher: Springer Nature, Singapore 2021 https://doi.org/10.1007/978-981-16-3641-7_1
14. Shojaati, M.; Beidokhti, B. Characterization of AISI 304/AISI 409 stainless steel joints using different filler materials. Construction and Building Materials **2017**, 147, 608–615 http://dx.doi.org/10.1016/j.conbuildmat.2017.04.185
15. Sun, Y.L; Obasi, G.; Hamelin, C.J.; Vasileiou, A.N.; Flinta, T.F.; Francis, J.A.; Smith, M.C. Characterization and modelling of tempering during multi-pass welding. Journal of Materials Processing Tech. 2019, 270, 118-131 https://doi.org/10.1016/j.jmatprotec.2019.02.015
16. Sun, Y.L Hamelin, C. J.; Vasileiou, A. N.; Xiong, Q.; Flint, T.F.; Obasi, G.; Francis, J.A.; Smith, M.C. Effects of dilution on the hardness and residual stresses in multipass steel weldments. International Journal of Pressure Vessels and Piping 187 (2020) 104154 https://doi.org/10.1016/j.ijpvp.2020.104154
17. Hsieh, C.-C.; Lin, Chen, M.-C.; Wu W. Microstructure, recrystallization, and mechanical property evolutions in the heat-affected and fusion zones of the dissimilar stainless steels. Materials Transactions **2007**, 48, 11 2898-2902. https://doi.org/10.2320/matertrans.MRA2007162
18. Hoang, A. T.; Le, V. V.; Nguyen, A. X. ; Nguyen, D. N. A study on the changes in microstructure and mechanical properties of multi-pass welding between 316 stainless steel and low-carbon steel. Journal of Advanced Manufacturing Technology **2018**, 12, 2, 25-40
19. Bahador, A.; Hamzah, E.; Mamat, M. F. Effect of filler metals on the mechanical properties of dissimilar welding of stainless steel 316L and carbon steel A516 GR 70. Jurnal Teknologi **2015**, 75, 7, 61–65 https://doi.org/10.11113/jt.v75.5174
20. Vargas, V.H.; Albiter, A.; Domínguez-Aguilar, M.A.; Altamirano, G.; Maldonado, C. Corrosion resistance of dissimilar GTA welds of pipeline steel and super duplex stainless steels in synthetic brine. Corrosion Iournal **2021**, 77, 6, 668-680 https://doi.org/10.5006/3746
21. Wang, J.; Lu. M.-x.; Zhang, L.; Chang, W.; Xu, Li-ning; Hu, L.-h. Effect of welding process on the microstructure and properties of dissimilar weld joints between low alloy steel and duplex stainless steel. International Journal of Minerals, Metallurgy and Materials **2012**, 19, 6, 518-524 https://doi.org/10.1007/s12613-012-0589-z
22. Ming, H.; Zhang, Z.; Wang, J.; E.-H., Han; Wang, P.; Sun, Z. Microstructure of a safe-end dissimilar metal weld joint (SA508-52-316L) prepared by narrow-gap GTAW. Materials Characterization **2017**,123, 233–243 http://dx.doi.org/10.1016/j.matchar.2016.11.029

23. Zhang, R.; Wu, Q.; Wang, L.; Zeng, C.; Wang, X. Study on A-TIG welding of Q245R/321 dissimilar steel. IOP Conf. Series: Earth and Environmental Science **2019**, 310 042011 https://doi.org/10.1088/1755-1315/310/4/042011
24. Yılmaz, R.; Tümer, M. Microstructural studies and impact toughness of dissimilar weldments between AISI 316 L and AH36 steels by FCAW. Int J Adv Manuf Technol **2013**, 67, 1433-1447 https://doi.org/10.1007/s00170-012-4579-0
25. Afriansyah, Arifin A. A. Dissimilar metal welding using Shielded metal arc welding: A Review. Technology Reports of Kansai University **2020**, 64, 04, 1935-1948
26. Bahandari, D.; Chhibberb, R.; Arorac, N.; Mehtad, R. Investigation of $TiO_2$–$SiO_2$–CaO–$CaF_2$ based electrode coatings on weld metal chemistry and mechanical behaviour of bimetallic welds. Journal of Manufacturing Processes **2016**, 23, 61-74 https://dx.doi.org/10.1016/j.jmapro.2016.05.013
27. Pratiwi, D.K.; Arifin, A.; Gunawan; Mardhi, A.; Afriansyah Investigation of welding parameters of dissimilar weld of SS316 and ASTM A36 joint using a grey-based Taguchi Optimization Approach J. Manuf. Mater. Process. **2023**, 7, 39 https://doi.org/10.3390/jmmp7010039
28. Mas, F.; Tassin, C.; Roch, F.; Yescas, M.; Todeschini, P.; Bréchet, Y. Growth morphologies and primary solidification modes in a dissimilar weld between a low-alloy steel and an austenitic stainless steel. Metals **2018**, 8, 284 : https://doi.org/10.3390/met8040284
29. Nivas, R.; Singh, P.K.; Das, G.; Das, S.K.; Kumar, S.; Mahato, B.; Sivaprasad, K.; Ghosh, M. A comparative study on microstructure and mechanical properties near interface for dissimilar materials during conventional V-grooveand narrow gap welding. Journal of Manufacturing Processes **2017**, 25, 274–283 http://dx.doi.org/10.1016/j.jmapro.2016.12.004
30. Asadollahi, A.; Bahrami, A.; Shamanian, M. The effects of filler metal and butter layer on the microstructure and mechanical properties of API 5L X65/AISI 304L joint. Journal of Materials Research and Technology **2023**, 23, 4148-4166 https://doi.org/10.1016/j.jmrt.2023.02.063
31. Ghosh, P. S.; Sen, A.; Chattopadhyaya, S.; Sharma, S.; Singh, J.; Li, C.; Królczyk, G.; Rajkumar, S. Progressive developments and challenges in dissimilar laser welding of steel to various other light alloys (Al/Ti/Mg): A comprehensive review. Heliyon **2022**, 8, e11710 https://doi.org/10.1016/j.heliyon.2022.e11710
32. Anawa, E.M.; Olabi, A.G. Optimization of tensile strength of ferritic/austenitic laser-welded components, Optics and Lasers in Engineering **2008**, 46, 571–577 https://doi.org/10.1016/j.optlaseng.2008.04.014
33. Casalino, G.; Guglielmi, P.; Lorusso, V.D.; Mortello, M.; Peyrec, P.; Sorgente, D. Laser offset welding of AZ31B magnesium alloy to 316 stainless steel. Journal of Materials Processing Technology **2017**, 242, 49–59 http://dx.doi.org/10.1016/j.jmatprotec.2016.11.020
34. Pereira, A. B.; Cabrinha, A.; Rocha, F.; Marques, P.; Fernandes, F. A. O.; Alves de Sousa, R. J. Dissimilar metals laser welding between DP1000 steel and aluminum alloy 1050. Metals **2019**, 9, 102 https://doi.org/10.3390/met9010102
35. Zhang, M.; Chen, G; Zhou, Y.; Liao, S. Optimization of deep penetration laser welding of thick stainless steel with a 10 kW fiber laser. Materials and Design **2014**, 53, 568–576 http://dx.doi.org/10.1016/j.matdes.2013.06.066
36. Stanciu, E. M.; Pascu, A.; Tierean, M. H.; Roata, I. C.; Voiculescu, I.; Hulka, I.; Croitoru, C. Dissimilar laser welding of AISI 321 and AISI 1010. Technical Gazette **2018**, 25, 2, 344-349 https://doi.org/10.17559/TV-20160722151049
37. Scutelnicu, E.; Iordachescu, M.; Rusu, C. C.; Mihailescu, D.; Ocaña, J. L. Metallurgical and mechanical characterization of low carbon steel - stainless steel dissimilar joints made by laser autogenous welding. Metals **2021**, 11, 810 https://doi.org/10.3390/met11050810
38. Venkatakrishna, A.; Lakshminarayanan, A.; Vasantharaja, P.; Vasudevan, M. Decisive impact of filler-free joining processes on the Microstructural evolution, tensile and impact properties of 9Cr-1Mo-V-Nb to 316 L(N) dissimilar joints. Proceedings of the Institution of Mechanical Engineers, Part C: Journal of Mechanical Engineering Science**. 2022**, 236, 5, 2408-2427 https://doi.org/10.1177/09544062211029307
39. Danielewski, H.; Skrzypczyk, A.; Tofil, S.; Witkowski, G.; Rutkowski, S. Numerical Simulation of Laser Welding Dissimilar Low Carbon and Austenitic Steel Joint. Open Eng. **2020**, 10. 491–498 https://doi.org/10.1515/eng-2020-0045
40. Hamada, A.; Ghosh, S.; Ali, M.; Jaskari, M.; Järvenpää. A. Studying the strengthening mechanisms and mechanical properties of dissimilar laser-welded butt joints of medium-Mn stainless steel and automotive

high-strength carbon steel. Materials Science & Engineering A **2022**, 856, 143936 https://doi.org/10.1016/j.msea.2022.143936

41. Hamada, A.; Khosravifard, A.; Ali, M.; Ghosh, S.; Jaskari, M.; Hietala, M.; Järvenpää, A.; Newishy, M. Micromechanical analysis and finite element modelling of laser-welded 5-mm-thick dissimilar joints between 316L stainless steel and low-alloyed ultra-high-strength steel. Materials Science & Engineering A **2023**, 882, 145442 https://doi.org/10.1016/j.msea.2023.145442
42. Prabakaran, M.P.; Kannan, G.R. Optimization of laser welding process parameters in dissimilar joint of stainless steel AISI316/AISI1018 low carbon steel to attain the maximum level of mechanical properties through PWHT. Optics and Laser Technology **2019**, 112, 314–322 https://doi.org/10.1016/j.optlastec.2018.11.035
43. Prabakaran, M.P.; Kannan, G.R. Effects of post-weld heat treatment on dissimilar laser welded joints of austenitic stainless steel to low carbon steel. International Journal of Pressure Vessels and Piping **2021**, 191, 104322 https://doi.org/10.1016/j.ijpvp.2021.104322
44. Liu, F.; Zhou, X.; Chen, X.; Gong, X.; Wu, L.; Chen, B.; Chen, K.; Tan, C. Melt flowing behaviors and microstructure evolution during laser offset welding of dissimilar metals between AH36 and 304 steels. Optics & Laser Technology **2022**, 151, 10802 https://doi.org/10.1016/j.optlastec.2022.108024
45. Li, G.; Zhang, C.; Gao, M.; Zeng, X. Role of arc mode in laser-metal active gas arc hybrid welding of mild steel. Materials and Design **2014**, 61, 239-250 http://dx.doi.org/10.1016/j.matdes.2014.04.079
46. Russo Spena, P.; Angelastro, A.; Casalino, G. Hybrid laser arc welding of dissimilar TWIP and DP high strength steel weld. Journal of Manufacturing Processes **2019**, 39 233–240 https://doi.org/10.1016/j.jmapro.2019.02.025
47. Zhang, X.; Mi, G.; Wang, C. Microstructure and performance of hybrid laser-arc welded high-strength low alloy steel and austenitic stainless steel dissimilar joint. Optics and Laser Technology **2020**, 122 105878 https://doi.org/10.1016/j.optlastec.2019.105878
48. Missori, S.; Sili, A. Prediction of weld metal microstructure in laser beam welded clad steel. Metallurgist, **2018**, 62, 84-92 https://doi.org/10.1007/s11015-018-0629-7
49. Salminen, A. The filler wire - laser beam interaction during laser welding with low alloyed steel filler wire. Mechanika. **2010**, 4, 84, 67-74
50. Hansen, K. S.; Olsen, F. O.; Kristiansen, M.; Madsen, O. Joining of multiple sheets in a butt-joint configuration using single pass laser welding with multiple spots. J. Laser Appl. **2015**, 27, 032011 https://doi.org/10.2351/1.4922222
51. Kristiansen, M.; Hansen, K. S.: Langbak, A.; Johansen, S. B.; Krempin, S. B.; Hornum, M. D. Single pass laser welding with multiple spots to join four sheets in a butt-joint configuration. Physics Procedia **2017**, 89, 205-213
52. Cui, L.; Chen, H.; Chen, B.; He, D. Welding of dissimilar steel/Al Joints using dual-beam lasers with side-by-side configuration. Metals **2018**, 8, 1017 https://doi.org/10.3390/met8121017
53. Xu, S.; Thermal stress analysis of dissimilar welding joints by finite element method. Procedia Engineering **2011**, 15, 3860 – 3864
54. Bharthi, A. D.; Babu, D. H. Structural and Thermal Analysis of Dissimilar Metal Welding of 1020 Mild Steel and 304 Stainless Steel. International Journal of Scientific Engineering and Technology Research **2015**, 04, 09, 1761-1771 https://doi.org/10.1016/j.matpr.2021.05.434
55. An, G.; Park, J.; Lim, W.; Park, H.; Han, I. Characteristics of welding residual stress distribution in dissimilar weld joints. Metals **2022**, 12, 405 https://doi.org/10.3390/met12030405
56. Dokme, F.; Kulekci, M.K.; Esme, U. Microstructural and mechanical characterization of dissimilar metal welding of Inconel 625 and AISI 316L, Metals **2018**, 8, 797 https://doi.org/10.3390/met8100797
57. Ramkumar, T.; Selvakumarb, M.; Narayanasamyc, P.; Ayisha Begamd, A.; Mathavand, P.; Arun Rajd, A. Studies on the structural property, mechanical relationships and corrosion behaviour of Inconel 718 and SS 316L dissimilar joints by TIG welding without using activated flux, J. of Manuf. Proc. **2017**, 30, 290-298 https://doi.org/10.1016/j.jmapro.2017.09.028
58. Shankar, V.; Gill, T.P.S.; Mannan, S.L.; Sundaresan, S. Solidification Cracking in Austenitic Stainless SteelWelds. Sadhana Acad. Proc. Eng. Sci. **2003**, 28, 359–382
59. Manitsas, D.; Andersson, J. Hot Cracking Mechanisms in Welding Metallurgy: A Review of Theoretical Approaches. In Proceendings of the ICEAF-V, Chios Island, Greece, 22–28 June 2018

60. Fei, Z.; Pan, Z.; Cuiuri, D.; Li, H.; Van Duin, S.; Yu, Z. Microstructural characterization and mechanical properties of K-TIG welded SAF2205/AISI316L dissimilar joint. Journal of Manufacturing Processes, **2019**, 45, 340-355 http://dx.doi.org/10.1016/j.jmapro.2019.07.017
61. Landowski, M.; ´Swierczynska, A.; Rogalski, G.; Fydrych, D. Autogenous fiber laser welding of 316L austenitic and 2304 lean duplex stainless steels. Materials **2020**, 13, 2930 https://doi.org/10.3390/ma13132930
62. Alali, M.; Abass, M. H.; Abbas, W. S.; Shehabd, A A. Effect of nickel powder buffering layer on microstructure and hardness properties of high carbon steel / stainless steel arc stud welding. Materials Research **2020**, 23, 1, e20190567 https://doi.org/10.1590/1980-5373-MR-2019-0567
63. Giudice, F.; Sili, A. Weld metal microstructure prediction in laser beam welding of austenitic stainless steel. Appl. Sci. **2021**, 11, 1463 https://doi.org/10.3390/app11041463
64. Tandon, V.; Patil, A. P.; Kowshik, S. Impact of filler electrodes on welding properties of dissimilar welded 316L/201 austenitic stainless steels. Eng. Proc. **2023**, 59, 90. https://doi.org/10.3390/engproc2023059090
65. Wu, C.; Li, S.; Zhang, C.; Wang, X. Microstructural evolution in 316LN austenitic stainless steel during solidification process under different cooling rates. J Mater Sci **2016**, 51, 2529–2539 https://doi.org/10.1007/s10853-015-9565-0
66. Zhai, R.; Zhang, H.; Xu, B.; Liu, S.; Xie, B.; Sun, M. Elimination of δ-ferrite in N50 steel and its effect on cryogenic mechanical properties. Cryogenics **2022**, 126 103522 https://doi.org/10.1016/j.cryogenics.2022.103522
67. Bunaziv, I.; Olden, V.; Akselsen, O.M. Metallurgical Aspects in the Welding of Clad Pipelines—A Global Outlook. Appl. Sci**. 2019**, 9, 3118 https://doi.org/10.3390/app9153118
68. Valiente Bermejo, M.A.: Reagent selection in austenitic stainless steel solidification modes characterization. Weld. J. **2012**, 91,133s–139s
69. Yu, P.; Thompson, K.J.; MCCarthy, J.; Kou, S. Microstructure evolution and solidification cracking in austenitic stainless steel. Welds. Weld. J. **2018**, 97, 301s–314s https://doi.org/10.29391/2018.97.026
70. Zhou, C.; Dia, P.; Wu, H.; He, M.; Liu, X.; Chu, P. K. Effect of the ferrite morphology on hydrogen embrittlement of MAG welded 304 austenitic stainless steel. Applied Surface Science **2022**, 606, 154866 https://doi.org/10.1016/j.apsusc.2022.154866
71. Wang, Q.; Chen, S.; Rong, L. Properties of heavy-section AISI 316 stainless steel casting. Metall Mater Trans **2020**, A 51, 2998–3008 https://doi.org/10.1007/s11661-020-05717-0
72. Weman, K. The weldability of steel (chap. 14) in Welding processes handbook, Woodhead Publishing Ltd, Cambridge, 2003, pp. 149-150
73. Tandon, V., Thombre, M.A., Patil, A.P. et al. Effect of Heat Input on the Microstructural, mechanical, and corrosion properties of dissimilar weldment of conventional austenitic stainless steel and low-nickel stainless steel. Metallogr. Microstruct. Anal. **2020**, 9, 668–677 https://doi.org/10.1007/s13632-020-00681-y
74. Vitek, J.M.; David, S.A.; Hinman, C.R. Improved Ferrite Number Prediction Model That Accounts for Cooling Rate Effects—Part 2: Model Results. Weld. J. **2003**, 82, 43s–50s
75. DuPont, J. N. Fundamentals of weld solidification, in *Metals Handbook*, 1st ed. Lienert, T. J.; Babu, S. S.; Siewert, T. A.; Acoff, V. L. Eds. ASM, Materials Park, Ohio US, 2011, Volume 06A, pp. 96-114
76. Ghosh, A., Misra, D., Acharyya, S.K.: Experimental and numerical investigation on laser welding of 2205 duplex stainless steel. Lasers Manuf. Mater. Process. **2019**, 6, 228–246 https://doi.org/10.1007/s40516-019-00090-2
77. Kik, T. Heat source models in numerical simulations of laser welding. Materials **2020**, 13, 2653
78. Giudice, F.; Missori, S.; Sili, A. Parameterized multipoint-line analytical modeling of a mobile heat source for thermal field prediction in laser beam welding. Int. J. Adv. Manuf. Technol. **2021**, 112, 1339–1358 https://doi.org/10.1007/s00170-020-06479-0
79. Giudice, F.; Sili, A. Validation of a theoretical model for laser welding thermal field by multi-physics numerical simulation. Metals **2023,** 13, 2020 https://doi.org/10.3390/met13122020
80. Gajjar, P. K.; Khatri, B. C.; Siddhpura, A.; Siddhpura, M. A. Sensitization and desensitization (healing) in austenitic stainless steel: A Critical Review. Trans Indian Inst Met **2022**, 75, 1411-1427 https://doi.org/10.1007/s12666-021-02439-8
81. Ramdan, R. D.; Kariem, M. A.; Neswan, O.; Wiriawan, F., Suratman, R.; Widyanto, B.; Wirawan, R. Mechanical properties and microstructure at stainless steel HAZ from dissimilar metal welding after heat treatment processes. IOP Conf. Series: Materials Science and Engineering **2019**, 553, 012034 https://doi.org/10.1088/1757-899X/553/1/012034

82. Dai, P.; Li, S.; Wu, L.; Wang, Y.; Feng, G. Dean Deng A new numerical model to predict welding-induced sensitization in SUS304 austenitic stainless steel joint. Journal of Materials Research and Technology **2022**, 17, 234e243 https://doi.org/10.1016/j.jmrt.2022.01.015
83. Winarto, W.; Anis, M.; Riastuti, R.; Suarjana, I.N. Study the effect of welding position and plate thickness to the mechanical and microstructural properties of the TIG dissimilar metal welded between carbon steel ASTM A36 and stainless steel 304 plates. Material Science Forum **2020**, 1000, 364–372 https://doi.org/10.4028/www.scientific.net/msf.1000.364
84. DuPont, J. N. Microstructural evolution and high temperature failure of ferritic to austenitic dissimilar welds. International Materials Reviews **2012**, 57, 4, 208-231 https://doi.org/10.1179/1743280412Y.0000000006
85. Nimko, M. O. Influence of welding parameters on decarburization in heat affected zone of dissimilar weldments after post weld heat treatment. Archives of Materials Science Engineering **2021**, 112, 1, 23-31 https://orcid.org/0000-0002-9672-4921
86. Britto, J. G.; Sulbihar, A. D.; Dinesh, K. L.; Jeya, J.; Durai R. R. B.; Sriram V. Microstructural studies of P91 and SS304L dissimilar welding. Materials Today: Proceedings **2021**, 47, 4571-4577